

## Magnetic Anisotropy of the Antiferroquadrupole Phase in $\text{Ce}_{0.50}\text{La}_{0.50}\text{B}_6$

Mitsuhiro Akatsu,<sup>1,\*</sup> Terutaka Goto,<sup>1</sup> Osamu Suzuki,<sup>2</sup> Yuichi Nemoto,<sup>1</sup> Shintaro Nakamura,<sup>3</sup>  
Satoru Kunii,<sup>4</sup> and Giyuu Kido<sup>2</sup>

<sup>1</sup>Graduate School of Science and Technology, Niigata University, Niigata 950-2181, Japan

<sup>2</sup>National Institute for Materials Science, 3-13 Sakura, Tsukuba 305-0003, Japan

<sup>3</sup>Center for Low Temperature Science, Tohoku University, Sendai 980-8577, Japan

<sup>4</sup>Department of Physics, Tohoku University, Sendai 980-8578, Japan

(Received 14 October 2003; published 8 October 2004)

Magnetic phase diagrams for antiferroquadrupole (AFQ) phase II and antiferromagnetic (AFM) phase III in  $\text{Ce}_{0.50}\text{La}_{0.50}\text{B}_6$  with a  $\Gamma_8$  ground state have been investigated by ultrasonic measurements. The hybrid magnet (Gama) in the National Institute for Materials Science was employed for high-field measurements up to 30 T and a  $^3\text{He}$ - $^4\text{He}$  dilution refrigerator was used for low-temperature experiments down to 20 mK. The phase boundary from paramagnetic phase I to AFQ phase II under [001] magnetic fields closes at  $H_{\text{I-II}} \sim 29$  T, while the boundary is still open under fields along the [110] and [111] directions even up to 30 T. This anisotropic character of phase II in fields is consistent with the theoretical calculation based on the  $O_{xy}$ -type AFQ ordering. We also found that AFM phase III reduces considerably in fields turning from the [001] to [110] and [111] directions.

DOI: 10.1103/PhysRevLett.93.156409

PACS numbers: 71.27.+a, 75.30.Gw, 75.30.Kz, 62.20.Dc

The spin and orbital degrees of freedom of  $4f$  electron in rare earth compounds brings about multipole orderings in addition to conventional magnetic dipole orderings at low temperatures. The Ce-based cubic compound  $\text{CeB}_6$  with a  $\Gamma_8$  quartet being mapped to  $\text{SU}(4)$  symmetry for the ground state, in particular, has currently received a lot of interest because of a rich variety of phenomena relating to multipole orderings. The separation of the  $\Gamma_8$  ground state from a  $\Gamma_7$  excited doublet at 540 K in  $\text{CeB}_6$  [1,2] provides an ideal electron system, which is dominated by the pure  $\Gamma_8$  quartet with 15 degrees of freedom of  $\text{SU}(4)$  as  $\Gamma_8 \otimes \Gamma_8 = \Gamma_1 \oplus \Gamma_2 \oplus \Gamma_3 \oplus 2\Gamma_4 \oplus 2\Gamma_5$ . Three magnetic dipoles of  $J_x, J_y, J_z$  with  $\Gamma_4$  symmetry are relevant for antiferromagnetic (AFM) ordering in phase III below  $T_N = 2.3$  K of  $\text{CeB}_6$ . There are five electric quadrupoles of  $O_2^0, O_2^2$  with  $\Gamma_3$  symmetry and  $O_{yz}, O_{zx}, O_{xy}$  with  $\Gamma_5$ . The intersite interaction of  $O_{yz}, O_{zx}, O_{xy}$  is relevant for the antiferroquadrupole (AFQ) ordering with a propagation vector  $\mathbf{k} = [1/2, 1/2, 1/2]$  in phase II below  $T_Q = 3.3$  K of  $\text{CeB}_6$  [3,4]. Seven magnetic octupoles consist of  $T_{xyz}$  with  $\Gamma_2$  symmetry,  $T_x^\alpha, T_y^\alpha, T_z^\alpha$  with  $\Gamma_4$ , and  $T_x^\beta, T_y^\beta, T_z^\beta$  with  $\Gamma_5$ . The octupole  $T_{xyz}$ , in particular, plays an important role to stabilize AFQ phase II of  $\text{CeB}_6$  under magnetic fields [4].

The transition temperature  $T_Q = 3.3$  K at zero field from paramagnetic phase I to AFQ phase II in  $\text{CeB}_6$  shifts to higher temperatures with increasing field as  $T_Q = 8.5$  K at  $H = 15$  T [3]. Recent high-field magnetic measurements with a metal film cantilever magnetometer revealed that the I-II phase transition temperature further increases to  $T_Q = 9.5$  K at 30 T [5]. A model calculation based on the Hamiltonian of the Ruderman-Kittel-Kasuya-Yoshida (RKKY)-type interaction for the  $O_{xy}$ -type quadrupole and field-induced octupole  $T_{xyz}$  has

successfully reproduced this increasing of  $T_Q$  with increasing field in  $\text{CeB}_6$  [6,7]. It has also been pointed out that the fluctuation of the multipole degrees of freedom of the  $\Gamma_8$  quartet plays a role in giving rise to the increase of  $T_Q$  with increasing field. Because of the symmetry breaking character of the AFQ ordering in phase II, the I-II phase boundary should definitely exist in magnetic field. Presumably, the I-II phase boundary in  $\text{CeB}_6$  is expected to show a closed loop in high magnetic fields. Recently, Shiina has shown an extended model calculation for the magnetic anisotropy of the AFQ phase in  $\text{CeB}_6$ . His calculation has shown that the I-II phase boundary may close at a high field of  $\sim 70$  T along the [001] direction and may not close even in fields of 70 T along the [110] or [111] directions [7]. Because of the difficulty of high-field experiments, the overall feature about AFQ phase II of  $\text{CeB}_6$  in fields has not been settled yet. The reduction of the intersite interactions in the diluted system  $\text{Ce}_x\text{La}_{1-x}\text{B}_6$  may provide a chance to detect whether the I-II phase boundary close or not with increasing field. The specific heat measurements on  $x = 0.4$ – $0.36$  in fields up to 15 T have shown a tendency to close the I-II phase boundary [8] that seems to be favorable for the theoretical anticipation by Shiina [7].

The decreasing  $x$  from pure  $\text{CeB}_6$  ( $x = 1.0$ ) in the diluted  $\text{Ce}_x\text{La}_{1-x}\text{B}_6$  system reduces the intersite quadrupole interaction for  $T_Q$  of AFQ phase II as well as the magnetic interaction for  $T_N$  of AFM phase III. The former quadrupole interaction decreases much faster than the latter magnetic interaction with decreasing  $x$ . The compound  $x = 0.75$  exhibits an ordered phase IV at  $T_C = 1.6$  K and successively changes into AFM phase III at  $T_N = 1.1$  K [9–11]. In magnetic fields phase IV closes to the tetracritical point where the I-II-III-IV phases coexist.

In diluted compounds of  $x = 0.70$  and  $0.65$  phase IV is stable down to 20 mK showing no sign of the transition to phase III [12]. The ordered phase IV is characterized by huge softening of the transverse  $C_{44}$  mode [9] and magnetic isotropy [10]. Recently, our group has found the transition from a cubic lattice to a trigonal one in phase IV with a spontaneous distortion  $\langle \varepsilon_{yz} \rangle = \langle \varepsilon_{zx} \rangle = \langle \varepsilon_{xy} \rangle \neq 0$ . We have proposed the ferroquadrupole ordering accompanied by trigonal distortion in phase IV [13]. The octupole ordering  $T_x^\beta, T_y^\beta, T_z^\beta$  with  $\Gamma_5$  symmetry in phase IV has also been proposed to explain the trigonal strain, which is proportional to the quadrupole, as the secondary order parameter [14].

In more diluted compounds  $x = 0.60$  and  $0.50$ , the  $\Gamma_8$  ground state falls into the nonmagnetic state due to the Kondo screening effect showing no distinct transition down to  $T = 0$  K [12,15,16]. The broad rounded anomaly around 1.0 K in specific heat in the compounds  $x = 0.60$  and  $0.50$  is distinguished from sharp  $\lambda$  peaks at the I-IV phase transition points in  $x = 0.70$  and  $0.75$  [15]. Furthermore, the low-temperature limit of the soft  $C_{44}$  in  $x = 0.60$  and  $0.50$  is shallower than that in phase IV of  $x = 0.70$  and  $0.75$  [12]. The low-temperature nonmagnetic state in  $x = 0.60$  and  $0.50$  easily transforms into the ordered AFQ phase II or AFM phase III in low-magnetic fields above  $H \sim 2$  T.

In the present Letter we report on the first observation of the upper critical field of phase II in  $x = 0.50$ , being responsible for the theoretical analysis of the intersite quadrupole interaction not only in  $x = 0.50$  but also in pure  $\text{CeB}_6$ . Furthermore, we report on a magnetic anisotropy of phase III at low temperatures. We have performed the ultrasonic measurements on the compound  $x = 0.50$  to examine the magnetic phase diagram at high magnetic fields up to 30 T and at low temperatures down to 20 mK. Single crystals of  $\text{Ce}_{0.50}\text{La}_{0.50}\text{B}_6$  for the present experiments were grown by a floating zone method. The hybrid magnet (Gama) consisting of the superconducting magnet and the water-cooled Cu magnet in the Tsukuba Magnet Laboratory at the National Institute for Materials Science was used for the present high-field ultrasonic measurements up to 30 T with a  $^4\text{He}$  cryostat. The temperature in high magnetic fields was measured by a calibrated thermometer of Cernox<sup>TM</sup> CX-1030AA (Lake Shore Cryotronics, Inc.), which is highly efficient against field-induced error [17]. The sensor in the present experiment indicates 1.8 K at 1.5 K and 30 T, which error reduces considerably in higher temperatures and below 20 T. A  $^3\text{He}$ - $^4\text{He}$  dilution refrigerator down to 20 mK with a top-loading probe combined to a superconducting magnet up to 18 T at Niigata University has been used for the low-temperature ultrasonic measurements. The temperature in the dilution refrigerator was measured by calibrated ruthenium oxide thermometers equipped at the side of a sample in the magnetic field center and the

mixing chamber in the field cancellation region. The ultrasonic pulse wave was generated and detected by piezoelectric plates  $\text{LiNbO}_3$  with thickness  $40 \mu\text{m}$  bonded on the plane parallel surfaces of the sample. The high electromechanical coupling coefficient  $k = 0.4\text{--}0.5$  in  $\text{LiNbO}_3$  was crucially important for low-input power ultrasonic experiments in the dilution refrigerator down to 20 mK.

Because the elastic constant corresponds to the quadrupole susceptibility, the ultrasonic measurement is a sensitive probe to detect the quadrupole phase transition of  $\text{Ce}_{0.50}\text{La}_{0.50}\text{B}_6$  in fields. In Fig. 1 we show the temperature dependence of the elastic constant  $C_{11}$  measured by the longitudinal ultrasonic wave propagating along the fourfold [001] axis. The magnetic fields up to 30 T were applied parallel to the propagation direction of [001]. The bending point indicating the I-II phase transition shifts to lower temperatures with increasing field from 15 T up to 25 T. The temperature dependence under 30 T, however, does not show any sign of the I-II phase transition above 1.8 K. This result clearly shows the I-II phase boundary closes at a critical field below 30 T. The inset of Fig. 1 shows  $\Delta C_{11}/C_{11}$  as a function of applied magnetic fields. At 1.5 and 3 K we have observed the I-II phase transition in low fields and successively the II-I phase transition in high fields. These transition points are shown by arrows in the inset of Fig. 1.

Next we survey the I-II phase transition points in fields along the threefold [111] axis and the twofold [110] axis, where phase II is expected to be more stable than that along [001]. In Fig. 2(a), we show the temperature dependence of  $C_{L[111]} = C_B + 4C_{44}/3$  in applied magnetic fields from 10 to 30 T along the [111] axis parallel to

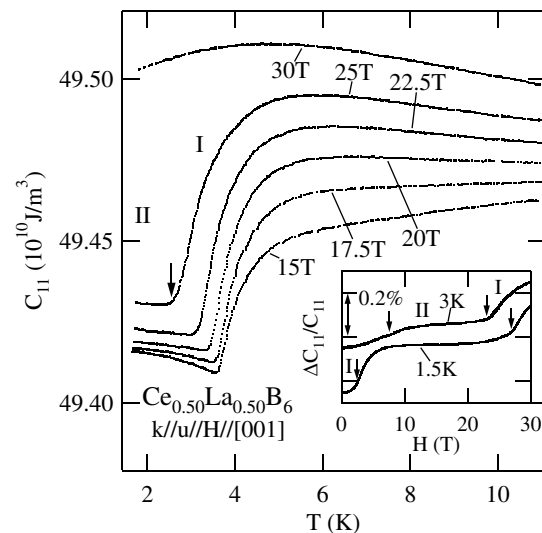


FIG. 1. Temperature dependence of the elastic constant  $C_{11}$  in  $\text{Ce}_{0.50}\text{La}_{0.50}\text{B}_6$  in high magnetic fields along the [001] direction. The inset shows field dependence of  $\Delta C_{11}/C_{11}$  at various temperatures.

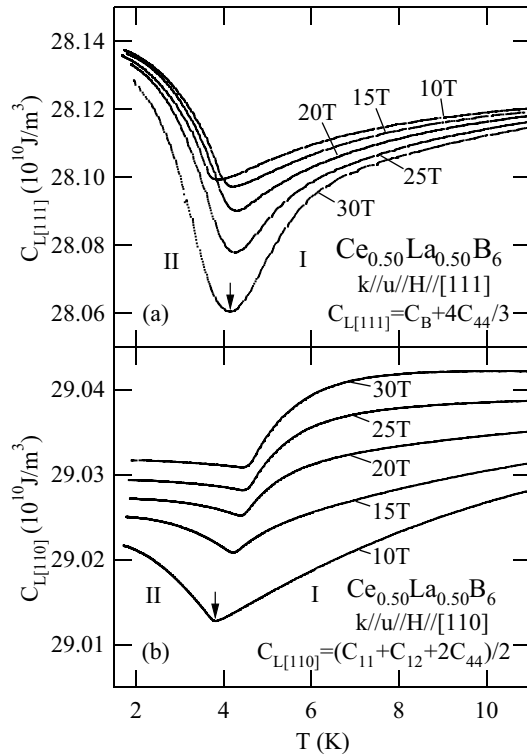


FIG. 2. (a) Temperature dependence of the elastic constant  $C_{L[111]} = C_B + 4C_{44}/3$  of  $Ce_{0.50}La_{0.50}B_6$  in high magnetic fields along the [111] direction. (b) Temperature dependence of the elastic constant  $C_{L[110]} = (C_{11} + C_{12} + 2C_{44})/2$  of  $Ce_{0.50}La_{0.50}B_6$  in high magnetic fields along the [110] direction.

the propagation direction of the longitudinal ultrasonic wave. The I-II phase transition temperature  $T_Q$  indicated by the minimum points shifts to higher temperatures with increasing field from 10 to 20 T. And above 20 T up to 30 T the  $T_Q$  turns to slightly decrease with increasing field.

In Fig. 2(b), we show the temperature dependence of  $C_{L[110]} = (C_{11} + C_{12} + 2C_{44})/2$  in applied magnetic fields along the [110] axis parallel to the propagation direction of the longitudinal ultrasonic wave. The bending point exhibiting the I-II phase transition shifts to higher temperatures with increasing field up to 25 T. The transition temperature to AFQ phase II from phase I at 30 T is almost equal to that at 25 T.

In Fig. 3 we show the field dependence of  $C_{44}$ ,  $(C_{11} - C_{12})/2$ , and  $C_{L[111]} = C_B + 4C_{44}/3$  at low temperatures in fields along the [001], [110], and [111] directions, respectively. The three elastic constants show the I-III phase transition with hysteresis at  $H \sim 1.8$  T. The  $C_{44}$  in  $H||[001]$  and  $C_{L[111]}$  in  $H||[111]$  clearly show anomalies of the III-II phase transition at  $H = 4.2$  T ( $T = 380$  mK) and 2.9 T ( $T = 29$  mK), respectively. The  $(C_{11} - C_{12})/2$  mode does not show an appreciable anomaly indicating the III-II phase transition in  $H||[110]$ . This result proba-

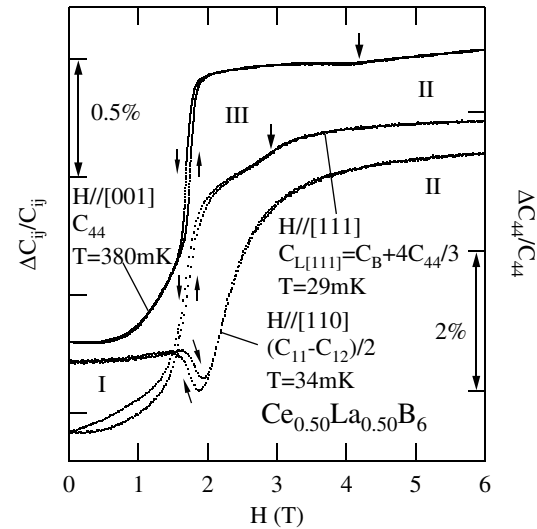


FIG. 3. Temperature dependence of the elastic constants  $C_{44}$ ,  $(C_{11} - C_{12})/2$ , and  $C_{L[111]} = C_B + 4C_{44}/3$  of  $Ce_{0.50}La_{0.50}B_6$  at low temperatures in applied magnetic fields along the [001], [110], and [111] directions, respectively.

bly means that the III-II phase transition point exists near the I-III phase transition point. The hysteresis behaviors near the I-III phase transition in Fig. 3 indicate that the I-III phase transition is a first order phase transition. The hysteresis behavior below  $H = 1.8$  T along the [111] direction may mean a magnetic induced short-range ordering occurs in low fields at low temperatures.

Figure 4 shows the magnetic phase diagrams of  $Ce_{0.50}La_{0.50}B_6$  in three applied magnetic fields along the [001], [111], and [110] directions. The solid symbols (circle, triangle, and square) indicate the phase transition points obtained by the present ultrasonic experiments. The open symbols (circle, triangle, and square) display the previous results of the ultrasonic and specific heat measurements [18]. The I-II phase transition point  $T_Q$  increases with increasing field up to 15 T. A tendency of the magnetic anisotropy  $T_{Q[001]} < T_{Q[111]} \sim T_{Q[110]}$  has already been observed in relatively low field below 15 T. As the magnetic fields along [001] increase above 15 T, the I-II phase transition point  $T_{Q[001]}$  decreases considerably and forms a closed loop with a critical field  $H_{I-II} \sim 29$  T at absolute zero. In fields along [111] and [110], however,  $T_{Q[111]}$  decreases and  $T_{Q[110]}$  increases slightly with increasing field above 20 T. The I-II phase boundaries along [111] and [110] do not show a closed loop even at 30 T. An appreciable difference in  $T_{Q[111]} = 4.1$  K and  $T_{Q[110]} = 4.5$  K at 30 T may promise the magnetic anisotropy of  $T_{Q[111]} < T_{Q[110]}$  in high magnetic fields above 15 T. The magnetic phase diagrams having a large anisotropy of  $T_{Q[001]} \ll T_{Q[111]} \sim T_{Q[110]}$  in high magnetic fields is almost duplicated by the theoretical calculation by Shiina in Ref. [7]. As was pointed out by Shiina *et al.*, the quite anisotropic Zeeman splitting of the  $\Gamma_8$

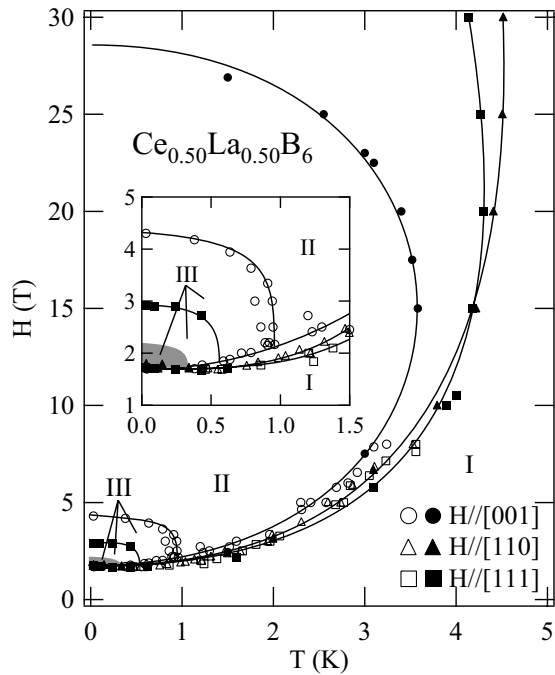


FIG. 4. Magnetic phase diagram of  $\text{Ce}_{0.50}\text{La}_{0.50}\text{B}_6$  in the applied magnetic field along the [001], [110], and [111] directions. The inset shows the low-temperature phase diagram of AFM phase III under fields along [001], [110], and [111].

quartet depending on the field directions accounts for the considerable anisotropy of  $T_{Q[001]} \ll T_{Q[111]} \sim T_{Q[110]}$  in high fields [19]. The theoretical calculation, however, cannot reproduce a small anisotropy of the experimental result  $T_{Q[111]} < T_{Q[110]}$ . One of the reasons is that the calculation did not take into account the magnetic induced dipole, although the quadrupoles  $O_{yz}$ ,  $O_{zx}$ ,  $O_{xy}$ , and octupole  $T_{xyz}$  were considered. The experimental determination of the magnetic anisotropy of AFQ phase II is very useful for the estimation of the RKKY-type intersite interaction in the system.

As one can see in the inset of Fig. 4, AFM phase III located inside AFQ phase II also shows anisotropic behavior in fields. At absolute zero phase III changes into phase II above the critical field of  $H_{\text{III-II}} = 4.3$  T in fields along the [001] direction. When the field is turned to the [111] direction, phase III shrinks considerably being the critical field of  $H_{\text{III-II}} = 2.9$  T for absolute zero. In the fields along the [110] direction, however, AFM phase III remains in the restricted region only, which is shown by the gray area in the inset. The magnetic anisotropy of phase III is supposed to be attributed to the complex magnetic structure and competition with multipole interaction [20,21]. On the other hand, the anisotropy of the I-III phase boundary at low temperatures is very small.

This fact suggests the Kondo screening effect depends hardly on magnetic directions.

In conclusion, we have successfully observed the magnetic anisotropy of AFQ phase II in  $\text{Ce}_{0.50}\text{La}_{0.50}\text{B}_6$  by using the hybrid magnet (Gama) up to 30 T. The I-II phase boundary of  $T_{Q[001]}$  in fields along the [001] direction shows a closed loop with the critical field  $H_{\text{I-II}} \sim 29$  T, which agrees with the phase boundary of the symmetry breaking character in Landau theory of phase transition. The anisotropy  $T_{Q[111]} < T_{Q[110]}$  in high magnetic fields above 15 T is of importance for the estimation of the intersite multipole interactions in the system. We have also found AFM phase III is stable in fields along the [001] direction and shrinks considerably in fields along [110], in particular. The high-field measurements with a pulse magnetic field above 30 T is required to observe a closed loop for the I-II phase boundary along the [110] or [111] direction.

We thank Dr. R. Shiina for stimulated discussions. The present work was supported by a Grant-in-Aid for Scientific Research from the Ministry of Education, Culture, Sports, Science and Technology of Japan.

\*Also at Nanoelectronics Research Institute, National Institute of Advanced Industrial Science and Technology, Tsukuba 305-8568, Japan.

- [1] E. Zirngiebl *et al.*, Phys. Rev. B **30**, 4052 (1984).
- [2] B. Lüthi *et al.*, Z. Phys. B **58**, 31 (1984).
- [3] J. M. Effantin *et al.*, J. Magn. Magn. Mater. **47&48**, 145 (1985).
- [4] O. Sakai *et al.*, J. Phys. Soc. Jpn. **66**, 3005 (1997).
- [5] D. Hall *et al.*, Phys. Rev. B **62**, 84 (2000).
- [6] R. Shiina, J. Phys. Soc. Jpn. **70**, 2746 (2001).
- [7] R. Shiina, J. Phys. Soc. Jpn. **71**, 2257 (2002).
- [8] M. Hiroi *et al.*, Phys. Rev. Lett. **81**, 2510 (1998).
- [9] O. Suzuki *et al.*, J. Phys. Soc. Jpn. **67**, 4243 (1998).
- [10] T. Tayama *et al.*, J. Phys. Soc. Jpn. **66**, 2268 (1997).
- [11] M. Hiroi *et al.*, J. Phys. Soc. Jpn. **66**, 1762 (1997).
- [12] Y. Nemoto *et al.*, Physica (Amsterdam) **31B2-313B**, 191 (2002).
- [13] M. Akatsu *et al.*, J. Phys. Soc. Jpn. **72**, 205 (2003).
- [14] K. Kubo and Y. Kuramoto, J. Phys. Soc. Jpn. **72**, 1859 (2003).
- [15] S. Nakamura *et al.*, Phys. Rev. B **61**, 15 203 (2000).
- [16] S. Nakamura *et al.*, Phys. Rev. B **68**, 100402 (2003).
- [17] B. L. Brandt *et al.*, Rev. Sci. Instrum. **70**, 104 (1999).
- [18] S. Nakamura *et al.*, J. Phys. Soc. Jpn. **64**, 3941 (1995); S. Nakamura *et al.*, *ibid.* **66**, 552 (1997); S. Nakamura *et al.* (unpublished).
- [19] R. Shiina *et al.*, J. Phys. Soc. Jpn. **66**, 1741 (1997).
- [20] H. Kusunose and Y. Kuramoto, J. Phys. Soc. Jpn. **70**, 1751 (2001); **70**, 3076 (2001).
- [21] Y. Kuramoto and K. Kubo, J. Phys. Soc. Jpn. **71**, 2633 (2002).